Inorganic Chemistry

pubs.acs.org/IC

Article

Thermodynamic Studies on the Hydrolysis of Trivalent Plutonium and Solubility of $Pu(OH)_3(am)$

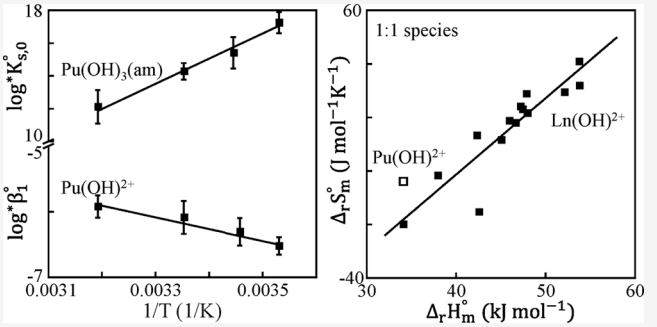
Sangki Cho, Hee-Kyung Kim, Tae-Hyeong Kim, Wansik Cha, and Hye-Ryun Cho*

Cite This: *Inorg. Chem.* 2022, 61, 12643−12651

Read Online

ACCESS | Metrics & More | Article Recommendations | Supporting Information

ABSTRACT: The temperature-dependent reaction properties of actinide elements are of particular interest in the safety assessment of high-level radioactive waste (HLRW) disposal systems. In this study, the hydrolysis of Pu(III) and the solubility of $Pu(OH)_3(am)$ were investigated at various temperatures (10−40 °C) in 0.1 M $NaClO_4$. A strong reducing condition for maintaining the oxidation state of Pu(III) while slowly increasing the pH of the solution was realized by electrolysis. The formation constants of the first hydrolysis species, log ${}^{*}\beta_1'$, and the solubility products of $Pu(OH)_3(am)$, log ${}^{*}K_{s,0}'$, at 10, 17, and 40 °C were experimentally determined using spectrophotometry, laser-induced breakdown detection, and radiometry. The enthalpy and entropy changes for these reactions were estimated using the van't Hoff equation. The first hydrolysis of Pu(III) is endothermic ($\Delta_r H_m^\circ$ = 34.10 ± 4.48 kJ mol^{-1}), and the dissolution of $Pu(OH)_3(am)$ is exothermic ($\Delta_r H_m^\circ$ = −294.29 ± 23.05 kJ mol^{-1}) with negative entropy changes. These thermodynamic data will contribute to improving the reliability of the safety assessment of HLRW disposal facilities and understanding the geochemical behavior of Pu under reducing or anoxic aqueous conditions at elevated temperatures.



Downloaded via LOS ALAMOS NATL LABORATORY on September 3, 2025 at 19:56:45 (UTC).
See https://pubs.acs.org/sharingguidelines for options on how to legitimately share published articles.

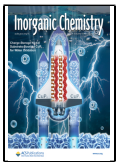
INTRODUCTION

Deep underground disposal systems have been considered in several countries for the final disposal of high-level radioactive waste (HLRW) such as spent nuclear fuel (SNF).[1] A safety assessment that satisfies the regulatory standards of each country is required prior to the construction and operation of a disposal facility; this assessment should be performed using a comprehensive model considering relevant scenarios including all features, events, and processes (FEPs) after HLRW repository closure. An important scenario to be considered is the release of radionuclides (RNs) due to the intrusion of groundwater through the multibarrier system of the repository.[2] For the reliable estimation of the geochemical behaviors and migration of RNs over a long time period, thermodynamic data for the reactions of RNs in aqueous solutions, such as solubility, redox reactions, hydrolysis, complexation, sorption, etc., are required. Several thermodynamic databases (TDBs) have been developed for this purpose.[3−6] The TDB project by OECD Nuclear Energy Agency (NEA) is renowned for the review and recommendation of reliable thermodynamic data; a second updated version of the chemical thermodynamic data of uranium, neptunium, plutonium, americium, and technetium has been recently published.[7]

In the early stage after the repository closure, the temperature around the disposal site is expected to increase owing to the decay heat of the HLRW.[8] For a reliable safety assessment and to understand the geochemical behaviors of RNs at elevated temperatures, the standard molal enthalpy and entropy changes of various reactions ($\Delta_r H_m^\circ$ and $\Delta_r S_m^\circ$) of RNs have been studied. However, reports on experimentally determined $\Delta_r H_m^\circ$ and $\Delta_r S_m^\circ$ for actinides are scarce, and there is an urgent need to explore the temperature-dependent chemistry of actinides, as emphasized in the last OECD-NEA review.[7] Recently, several research groups in the field of actinide chemistry focused on this research theme; this led to an increase in the available thermodynamic data for actinides such as Am/Cm,[9,10] Np,[11,12] and U.[13−16]

Pu is one of the most important radioactive elements. SNF contains approximately 1 wt % of Pu which is second only to U as a single element contributor to SNF.[17] Despite relatively minor contribution to the total radiotoxicity in the short term time scale of 100 years, the radiotoxicity contribution of Pu is significant because it becomes dominant over time, due to the long-lived isotopes of ^{239}Pu with a half-life of 24 000 years.[18] Therefore, it is important to gain a precise understanding of the chemical and physical behaviors of Pu under the long-term

Received: May 9, 2022
Published: August 3, 2022



© 2022 American Chemical Society

https://doi.org/10.1021/acs.inorgchem.2c01590
Inorg. Chem. 2022, 61, 12643−12651

evolution of underground disposal environments similar to what we have achieved for other actinides such as U, Np, Am, and Cm.

Pu(III) and Pu(IV) are expected to coexist in the reducing conditions of underground repositories owing to the major contribution of the anoxic corrosion of metallic iron utilized for making the waste container, with additional effects of radiolysis, microbial respiration, and reducing minerals.[19,20] However, reliable experimental studies on the chemical thermodynamics of aqueous Pu(III) species are limited because of the redox reactions of Pu in solutions. Over the past few decades, the hydrolysis of Pu(III) and the solubility of Pu(III) compounds at ambient temperature have been studied[21−23] and comprehensively reviewed in the literature.[7,20] The stability of $Pu(OH)_3(s)$ has been discussed by Neck et al.;[20] they concluded that $Pu(OH)_3(s)$ was only stable up to the redox condition of (pe + pH) = (−0.4 ± 1.0), which is not in the stability field of water [0 < (pe + pH) < 20.77], where the log ${}^{*}K^{\circ}_{s,0}$ = 15.8 ± 0.8 determined by Felmy et al.[21] was adopted. In our previous work, the hydrolysis of Pu(III) and the solubility of $Pu(OH)_3$(am) were studied under strong reducing conditions at 25 °C.[22] The results indicated that $Pu(OH)_3$(am) was stable in aqueous solutions up to the redox condition of (pe + pH) = (0.8 ± 0.5). Tasi et al. reported the solubility of PuO_2(ncr, hyd) in the pH range 8 < pH < 13 under reducing conditions achieved using $SnCl_2$ (pe + pH = 2); the reduction of Pu(IV) and generation of the solid phase of Pu(III) were confirmed by X-ray absorption near edge structure (XANES).[23] However, the $\Delta_r H^{\circ}_m$ and $\Delta_r S^{\circ}_m$ for the hydrolysis and dissolution reactions of trivalent actinides [Pu(III) and Am/Cm(III)] have not been reported;[7] only the $\Delta_f H^{\circ}_m$ of $Am(OH)_3(s)$, determined using a microcalorimeter, has been reported so far.[24]

The purpose of this work is to experimentally determine the thermodynamic data of Pu(III) hydrolysis at various temperatures. Our previous investigation at 25 °C[22] was systematically extended to study the hydrolysis of Pu(III) and the solubility of $Pu(OH)_3$(am) at T = 10, 17, and 40 °C. To maintain strong reducing conditions and increase the pH, coulometric titration was employed. The concentration of hydrated Pu^{3+} ions was determined using a spectrophotometer; the solubility study was accompanied by the detection of colloidal nanoparticles using a laser-induced breakdown detection (LIBD) system. Liquid scintillation counting (LSC) was used to determine the concentrations of dissolved Pu in the solutions after phase separation using ultrafiltration. Temperature-dependent values of log ${}^{*}\beta'_1$ and log ${}^{*}K'_{s,0}$ at 10, 17, 25, and 40 °C were determined and extrapolated into log ${}^{*}\beta^{\circ}_1$ and log ${}^{*}K^{\circ}_{s,0}$ under extremely dilute conditions (I = 0 M) based on the specific ion interaction theory (SIT).[25] The values of $\Delta_r H^{\circ}_m$ and $\Delta_r S^{\circ}_m$ were calculated for this system using the van't Hoff equation.

EXPERIMENTAL SECTION

Sample Preparation. All concentrations given by the molar concentration scale (M, mol/L) were measured at ambient temperature. The experimental ionic strength of 0.1 M $NaClO_4$ is considered to be 0.1 molal concentration (m, mol/kg), as the conversion factor at 0.1 M $NaClO_4$ is only 1.0075, and the change in the molar concentration of 0.1 M $NaClO_4$ solution induced by the variation in temperature from 10 to 40 °C is less than 1%.[26,27] All solutions were prepared using ultrapure water (18.2 MΩ cm, Millipore) and kept in a glovebox filled with argon gas (O_2 < 10 ppm). $NaClO_4$ salt (ACS grade, Sigma-Aldrich) was purified by recrystallization, and perchloric acid (TraceSELECT, Fluka) was used as purchased. The purification and preparation of Pu stock solutions and an electrolysis setup for preparing Pu(III) samples and controlling reducing conditions have been described in detail elsewhere.[22] A dissolved solution of PuO_2 (^{242}Pu, 99.932%, ORNL) was purified by anion exchange chromatography, and a Pu(VI) stock solution was prepared by evaporating it to dryness with concentrated $HClO_4$ and dissolving the dried sample in 1 M $HClO_4$. Pu(VI) was reduced to Pu(III) by electrolysis using a three-electrode system [Pt gauze as the working and counter electrodes and a Ag/AgCl reference electrode (RE-5B, BASi)] in a glovebox. The oxidation state of Pu in the stock solution was confirmed by spectrophotometry. The absence of colloidal contamination in the background materials (5.77 ± 0.02 M $NaClO_4$ and 1.0 M $HClO_4$) and Pu(III) stock solutions in 1 M $HClO_4$ was confirmed using LIBD. The initial 20 mL of Pu sample in 0.1 M $NaClO_4$ was prepared in a Teflon vessel by appropriate dilution of the Pu(III) stock solution with a 0.1 M $NaClO_4$ solution. The initial concentrations of Pu samples were in the range from 0.02 to 0.2 mM at pH 3.4−2.4. Hydrogen ions were reduced to hydrogen gas ($H^+ + e^- \rightarrow \frac{1}{2}H_2$) by electrolysis, which resulted in an increase in pH without changes in the concentration and oxidation state of Pu. A constant negative voltage was applied for at least 12 h under magnetic stirring to increase the pH. For example, at 10 °C, the pH value of the sample solution in 20 mL increased from 4.9 to 5.2 by electrolysis at −0.46 V for 18 h. Electrolysis for approximately 3 weeks increased the pH of the initial Pu sample from 2.7 to 8.3. It is expected that an equilibrium state is reached during an extremely slow increase of pH by electrolysis. Normally, additional equilibrating time is not necessary.[22] For the experiments at 10 and 17 °C, the samples were equilibrated for 3−4 h before every measurement of pH, absorption spectra, and LIBD. All measurements at 40 °C were carried out after a short waiting time of 5−10 min, considering the relatively fast kinetics of oxidation at high temperatures (see Figure S1). During electrolysis, a constant temperature was maintained by thermostatic water circulation around the Teflon electrolysis vessel, as described in our previous work.[22]

Spectrophotometry. Absorption spectra in the visible−NIR wavelength range were measured using a spectrophotometer (CARY5000, Agilent). A sealable quartz cell (Macro 117.100F, Hellma) with an optical path length of 1 cm and a liquid waveguide capillary cell (LWCC-3100, WPI) of 100 cm were used. The capillary cell was installed in a glovebox and coupled with the spectrophotometer using optical fibers as described in detail elsewhere.[28] A Peltier-thermostated multicell holder (G9840AA for CARY5000, Agilent) was employed to control the temperature of Pu samples in a quartz cell during absorption measurements; the temperature was set from 10 to 100 °C and monitored with a temperature probe inserted into a water-filled quartz cell. The temperature of the samples in the capillary cell was controlled by circulating thermostatic water at 10, 17, and 40 °C around the capillary cell. Absorption spectra in the range 400−850 nm for a quartz cell and 400−700 nm for a capillary cell were recorded at 1 nm intervals, a 60 nm/min scan rate, and a 3 nm spectral bandwidth. The spectrum from 520 to 630 nm was deconvoluted using Fityk software (least-squares curve fitting) based on the Voigt function.

Liquid Scintillation Counting. A liquid scintillation counter (Tri-Carb 3110-TR, Packard) with an α/β discriminator was employed to determine the total concentration of Pu. An aliquot of the Pu sample was mixed with 15 mL of cocktail (Ultima Gold AB, PerkinElmer). The activity of ^{242}Pu was 86.5% of the total alpha activity (11.7% for ^{238}Pu, 1.2% for ^{239}Pu, and ^{240}Pu, 0.6% for ^{241}Am), based on the certified isotopic inventory of Pu. For the Pu samples at high pH, where colloidal nanoparticles or precipitates were formed, phase separation was conducted by ultrafiltration (10 kDa, Ultracel YM regenerated cellulose membrane, Centricon-10, Millipore) at the same temperature at which the experiments were performed, and the concentrations of dissolved Pu were measured by LSC.

Monitoring the Formation of Colloidal Nanoparticles. The trace amounts of colloidal particles generated by Pu hydrolysis were monitored using an LIBD system; the details have been described elsewhere.[29] A temperature-controlled cuvette holder (Peltier-type, Model No. F7000, Quantum Northwest Inc.) was used to maintain the temperature of the samples during the LIBD measurements. The

https://doi.org/10.1021/acs.inorgchem.2c01590
Inorg. Chem. 2022, 61, 12643−12651

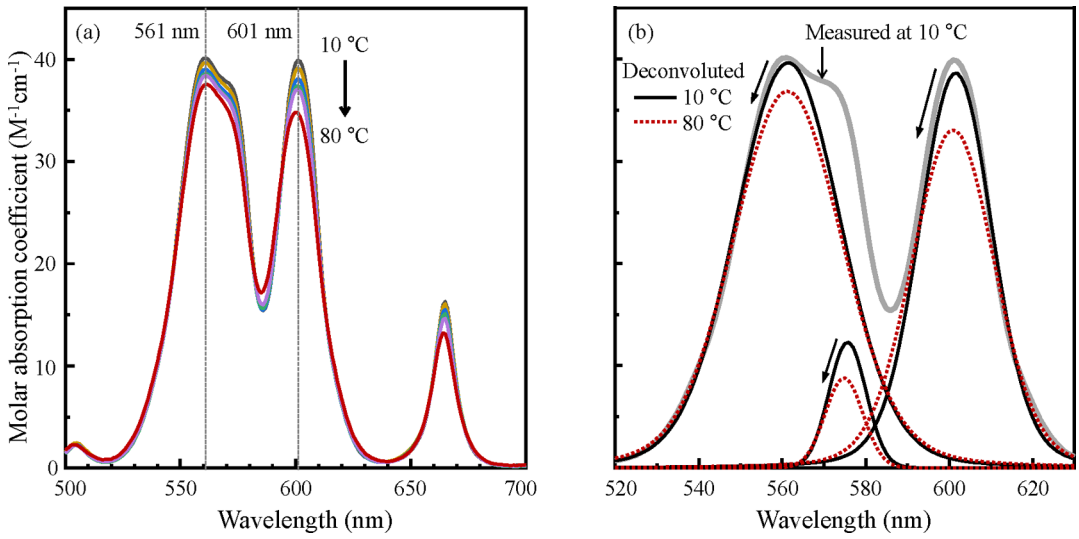


Figure 1. (a) Absorption spectra of Pu(III) in 0.1 M $HClO_4$ were recorded as a function of temperature. The dashed lines show absorption peaks of 561 and 601 nm at 25 °C. (b) Deconvoluted peaks of the measured spectra at 10 °C (solid lines) and 80 °C (dotted lines) are compared. A thick line shows the measured spectrum at 10 °C; the spectrum at 80 °C is not shown.

formation of colloids was determined by comparing the LIBD signals with those for 0.1 M $NaClO_4$ solutions.

pH Measurements. pH measurements using a pH electrode are affected by ionic strength, temperature, and background electrolyte property of sample solutions.[30] The relationship between measured pH (pH_{meas}) and the hydrogen ion concentration ($pH_c = -\log[H^+]$) can be described by eq 1:

$$pH_c = pH_{meas} + A_c \tag{1}$$

$$A_c = \log \gamma_{H^+} + \Delta E_j(F/RT \ln 10) \tag{2}$$

where F, R, and T are the Faraday constant (96 485 C mol^{-1}), universal gas constant (8.314 J K^{-1} mol^{-1}), and temperature in Kelvin, respectively. The term A_c is an empirically determined factor involving the effects of the activity coefficient of the hydrogen ion (γ_{H^+}) and a liquid-junction potential between the internal electrolyte and electrolyte of sample solutions (ΔE_j).[31] To determine the pH_c of a Pu sample, the pH_{meas} of the sample was measured with a Ross-type combination pH electrode (8103BN, Semimicro, glass body, Orion, Thermo Scientific) filled with 1.0 M $NaClO_4$. The pH electrode was calibrated using pH standards (pH 1.68, 4.01, 7.00, and 10.01, Thermo Fisher Scientific) at a constant temperature (10, 17, 25, and 40 °C). Based on eq 1, pH_c values were calculated using pH_{meas} and the experimentally obtained factor, A_c. The temperature-dependent A_c values for Na/$HClO_4$ solution at an ionic strength of 0.1 m were 0.021, 0.009, 0.002, and −0.027 at 10, 17, 25, and 40 °C, respectively. The measured A_c values at various ionic strengths (0.1−3.0 m) are described in the Supporting Information (Tables S1−S4 and Figure S2).

Thermodynamic Calculations. The formation constant, ${}^*\beta'_n$, and solubility product, ${}^*K'_{s,0}$, were determined according to eqs 3 and 4, respectively:

$${}^*\beta'_n = [Pu(OH)_n^{3-n}][H^+]^n/[Pu^{3+}] \tag{3}$$

for $Pu^{3+} + nH_2O \rightleftharpoons Pu(OH)_n^{3-n} + nH^+$

$${}^*K'_{s,0} = [Pu^{3+}]/[H^+]^3 \tag{4}$$

for $Pu(OH)_3(s) + 3H^+ \rightleftharpoons Pu^{3+} + 3H_2O$.

The conditional equilibrium constants, ${}^*\beta'_1$ and ${}^*K'_{s,0}$ at an ionic strength of 0.1 m $NaClO_4$ with varied temperature, are extrapolated to zero ionic strength with the SIT as described in the literature (eqs 5 and 6):[25]

$$\log K' - \Delta z^2 D = \log K^\circ + \Delta\varepsilon I \tag{5}$$

$$D = \frac{A\sqrt{I_m}}{1 + Ba_j\sqrt{I_m}} \tag{6}$$

where $\Delta z^2 = \{\sum (z_{products}{}^2) - \sum (z_{reactants}{}^2)\}$, z is the charge for each ion in the reaction, D is the temperature-dependent Debye−Hückel term, and $\Delta\varepsilon$ is the stoichiometric sum of the binary ion−ion interaction coefficients. A is the temperature-dependent Debye−Hückel constant listed in NEA-TDB,[7] and the constant A at 17 °C, where the experiment was conducted, was approximated by the value at the adjacent temperature of 15 °C. The Debye−Hückel term Ba_j is assigned as a constant value of 1.5 $kg^{1/2}$ $mol^{-1/2}$ with a small error of ±0.01 $kg^{1/2}$ $mol^{-1/2}$ below 100 °C. The ion interaction parameters $\varepsilon(j, k, I_m)$ have been considered almost independent of temperature with a slight variation of $(\partial\varepsilon/\partial T)_p \leq 0.005$ kg mol^{-1} K^{-1} below 200 °C.[7] Ion interaction parameters of $\varepsilon(Pu^{3+}; ClO_4^-) = 0.49 \pm 0.05$, $\varepsilon(Pu(OH)^{2+}; ClO_4^-) = 0.39 \pm 0.04$ from the $\varepsilon(Am(OH)^{2+}; ClO_4^-)$ as an analogue, and $\varepsilon(H^+; ClO_4^-) = 0.14 \pm 0.02$ listed in the literature[7] were used. The uncertainties of ${}^*\beta^\circ_1$ and ${}^*K^\circ_{s,0}$ were calculated based on the rules of error propagation $[\sigma^2_{\log K} = \sigma'^2_{\log K} + (m_{ClO_4^-}\sigma_{\Delta\varepsilon})^2]$.

With the small temperature variation of 10−40 °C in the present work, the molar heat capacity of the reaction $\Delta_r C^\circ_{p,m}$ is assumed to be zero; therefore, the change in the standard molar enthalpy $\Delta_r H^\circ_m$ is considered to be constant.[32] For the evaluation of the temperature dependency of the hydrolysis of Pu(III) and the solubility of $Pu(OH)_3(s)$, thermodynamic parameters ($\Delta_r H^\circ_m$ and $\Delta_r S^\circ_m$) of the reactions were determined using the integrated van't Hoff equation:

$$\log K^\circ(T) = \log K^\circ(T_0) + \frac{\Delta_r H^\circ_m(T_0)}{R \ln 10}\left(\frac{1}{T_0} - \frac{1}{T}\right) \tag{7}$$

where R is the universal gas constant (8.314 J K^{-1} mol^{-1}), and T is the temperature in Kelvin.

RESULTS AND DISCUSSION

Absorption Spectra. Figure 1a shows the absorption spectra of the reference Pu(III) solutions in 0.1 M $HClO_4$ as a function of temperature. At 25 °C, absorption peaks centered at 561, 601, and 665 nm were observed with molar absorption coefficients of 39.0 ± 0.6, 38.2 ± 0.6, and 15.2 ± 0.3 M^{-1} cm^{-1}, respectively, in good agreement with the values reported by Cohen (ε = 38 and 38 M^{-1} cm^{-1} at 561 and 601 nm).[33] With an

https://doi.org/10.1021/acs.inorgchem.2c01590
Inorg. Chem. 2022, 61, 12643−12651

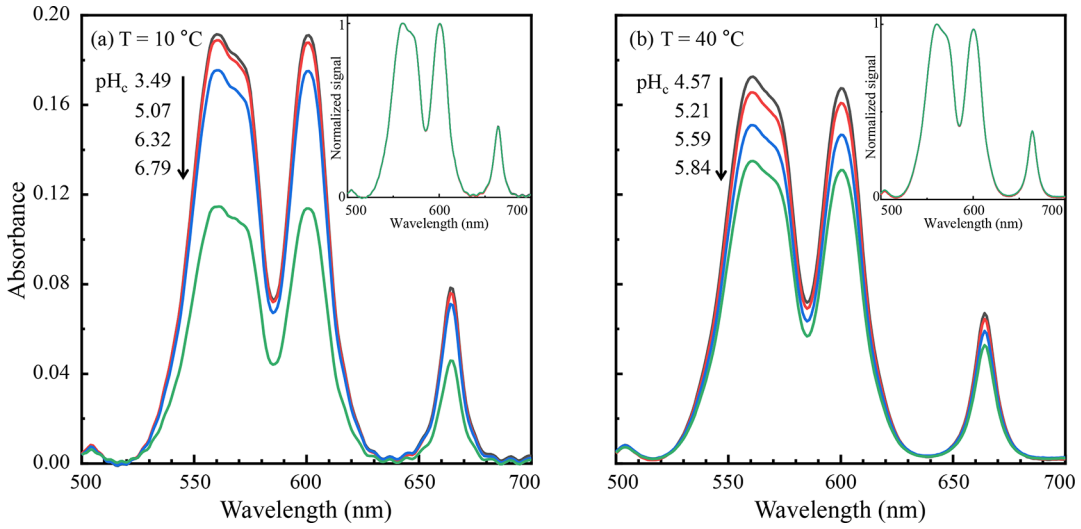


Figure 2. Absorption spectra of Pu(III) samples were measured at 10 (a) and 40 °C (b). These samples have no colloidal particles as confirmed using LIBD (I = 0.1 M $NaClO_4$). The normalized spectra are displayed in the insets.

increase in temperature from 10 to 80 °C, molar absorption coefficients at 561 and 601 nm decreased from 40.2 ± 0.2 to 37.6 ± 0.7 and from 39.9 ± 0.1 to 34.8 ± 0.6 M^{-1} cm^{-1}, respectively. The molar absorption spectrum at each temperature was obtained by averaging the absorption spectra of several Pu(III) solutions in 0.1 M $HClO_4$ with different Pu concentrations.

To further investigate the temperature-dependent changes in the peak positions and molar absorption coefficients, the spectra between 520 and 630 nm were deconvoluted until they converged to a constant value of the weighted square sum of the residuals. The deconvoluted peaks at 561, 576, and 602 nm with molar absorption coefficients of 39.7, 12.3, and 36.7 M^{-1} cm^{-1} at 10 °C altered to 561, 575, and 601 nm, with molar absorption coefficients of 37.5, 9.5, and 32.9 M^{-1} cm^{-1} at 80 °C, as displayed in Figure 1b. With increasing temperature, the deconvoluted peaks at 561 and 601 nm consistently showed a decrease in the molar absorption coefficient and hypsochromic shift within 1 nm. These observations might be attributed to temperature-dependent solvent effects, such as a decrease in the number of water molecules in the outer hydration sphere and the polarity changes of water molecules.[34]

Figure 2 shows the representative absorption spectra of Pu(III) samples at various pH values at two different temperatures of 10 and 40 °C, with the normalized absorption spectra shown in the insets. The total Pu concentrations of 0.048 mM (Figure 2a, T = 10 °C) and 0.045 mM (Figure 2b, T = 40 °C) remained constant while increasing pH; however, the absorbance of Pu(III) decreased with no change in spectral shapes as shown in the insets of Figure 2. The concentrations of the dissolved Pu(IV), Pu(V), and Pu(VI) species were lower than the limit of detection (0.1−0.4 μM) by spectrophotometry using a capillary cell,[22] and the solid phase including colloidal nanoparticles was not formed as confirmed by the LIBD measurements (see Figure S3). Therefore, plutonium in these samples depicted in Figure 2 existed in the form of dissolved Pu(III) species, which are hydrated Pu^{3+} ions and Pu(III) hydrolysis species. The concentrations of hydrated Pu^{3+} ions ($[Pu^{3+}]$) were directly determined by spectrophotometry at each temperature using the reference spectrum shown in Figure 1a under an assumption that the molar absorption coefficient of the Pu(III)−OH species from 500 to 700 nm was close to zero as suggested in our previous work.[22] As observed in Figure 2a,b, $[Pu^{3+}]$ decreased from 0.048 to 0.029 mM with the increase of pH$_c$ from 3.49 to 6.79 at 10 °C and from 0.045 to 0.035 mM with the pH$_c$ increase from 4.57 to 5.84 at 40 °C. The decreased $[Pu^{3+}]$ is regarded as proof of the equivalent generation of Pu(III)−OH species in these samples.

Hydrolysis of Pu(III). Figure 3 shows the result of a slope analysis according to the relationship of $\log(\sum[Pu(OH)_n^{3-n}]/$

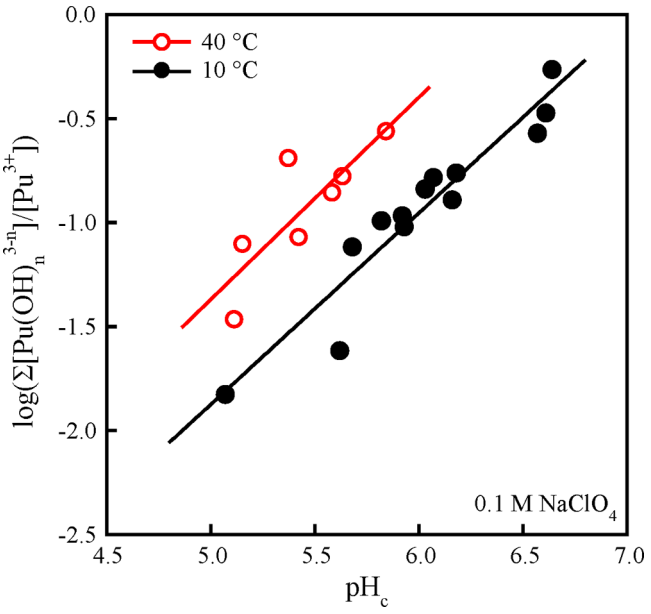


Figure 3. Plots of $\log(\sum [Pu(OH)_n^{3-n}]/[Pu^{3+}])$ vs pH$_c$ and linear regression analyses at T = 10 and 40 °C (I = 0.1 M $NaClO_4$).

$[Pu^{3+}])$ vs pH$_c$ for verifying the dominant hydrolyzed species. The concentration of the hydrolysis species, $\sum[Pu(OH)_n^{3-n}]$, was calculated using eq 8:

$$[Pu]_{tot} = [Pu^{3+}] + \sum [Pu(OH)_n^{3-n}] \quad (8)$$

where $[Pu]_{tot}$ is the initial Pu concentration measured under acidic conditions, and $[Pu^{3+}]$ is determined by spectrophotometry. None of the samples had detectable dissolved Pu(IV),

https://doi.org/10.1021/acs.inorgchem.2c01590
Inorg. Chem. 2022, 61, 12643−12651

Table 1. First Hydrolysis Constants for the Reaction $Pu^{3+} + H_2O \rightleftharpoons Pu(OH)^{2+} + H^+$ at 10, 17, 25, and 40 °C

temperature (°C)	log ${}^*\beta_1'$ (I = 0.1 M $NaClO_4$)	log ${}^*\beta_1^\circ$ (I = 0 M, SIT)	$\Delta_r H_m^\circ$ (kJ mol^{-1})	$\Delta_r S_m^\circ$ (J mol^{-1} K^{-1})
10	−6.97 ± 0.13	−6.52 ± 0.13		
17	−6.75 ± 0.21	−6.31 ± 0.21	34.10 ± 4.48	−3.91 ± 15.28
25	−6.53 ± 0.25[a]	−6.09 ± 0.25[a]		
40	−6.38 ± 0.17	−5.92 ± 0.17		

[a]Recalculated value from ref 22.

Pu(V), and Pu(VI) species, and there were no colloidal particles, as confirmed by spectrophotometry coupled with a capillary cell and LIBD. A linear correlation with the slopes of 0.92 ± 0.09, 1.06 ± 0.22, and 0.97 ± 0.29 was observed at 10, 17, and 40 °C, respectively. For clarity, the data at 17 °C are separately shown in Figure S4. Slopes close to 1 indicate that the first hydrolyzed species, $Pu(OH)^{2+}$, was dominant in these samples.

Based on $[Pu^{3+}]$ determined by spectrophotometry, $[Pu(OH)^{2+}]$ (=$[Pu]_{tot} - [Pu^{3+}]$ (eq 8), n = 1)) and pH_c, the first hydrolysis constants of Pu(III) at an ionic strength of 0.1 M $NaClO_4$ were determined at 10, 17, and 40 °C, as listed in Table 1. All of the information on $[Pu^{3+}]$ and $[Pu(OH)^{2+}]$ at each pH_c and temperature is summarized in Table A1 of the Appendix.

The previously reported log ${}^*\beta_1'$ and log ${}^*\beta_1^\circ$ values at 25 °C by our group[22] were recalculated considering the A_c factor of 0.002 determined in this work and listed in Table 1.

The species distribution of the experimentally determined Pu^{3+} ions and $Pu(OH)^{2+}$ and the calculated curves with the formation constants at 10, 17, and 40 °C are shown as a function of pH_c in Figure 4. At higher temperatures, the first hydrolysis species was formed at lower pH_c values. The calculated species fraction of 0.5 at 10, 17, and 40 °C appeared at pH_c values of 7.0, 6.7, and 6.4, respectively.

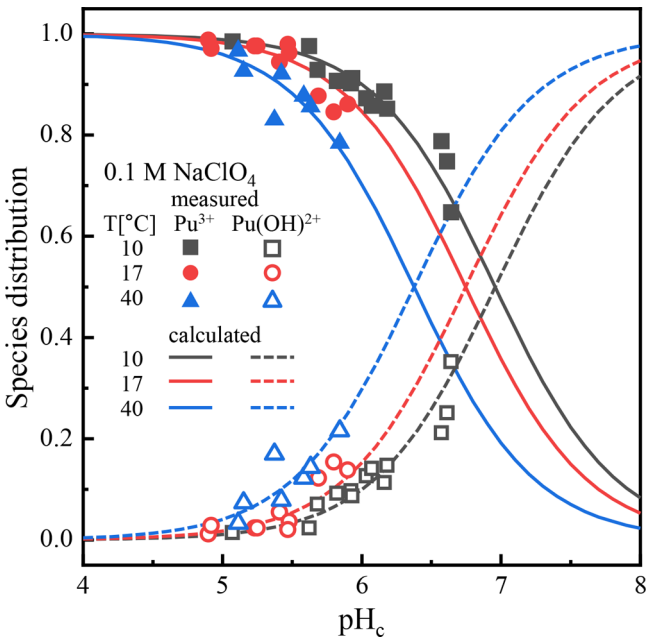


Figure 4. Species distributions of Pu^{3+} (closed symbols and solid lines) and $Pu(OH)^{2+}$ (open symbols and dashed lines) displayed as a function of pH_c. The symbols represent the experimental data, and the lines are calculated fractions from the formation constants (${}^*\beta_1'$) obtained in this work.

Solubility of $Pu(OH)_3$(am). The temperature-dependent solubility of Pu(III) hydrolyzed compounds was investigated under high pH conditions, where colloidal nanoparticles of $Pu(OH)_3$(s) were generated and detected by LIBD (see Figure S5). The solubility products were found using eq 4 with the spectrophotometrically determined $[Pu^{3+}]$ and pH_c for samples that contained detectable amounts of Pu^{3+} ions in aqueous solutions. For samples that contained too low $[Pu^{3+}]$ to be detected by absorption spectroscopy using a capillary cell, the concentration of dissolved Pu ($[Pu_{dis}]$) was determined by LSC after phase separation by ultrafiltration. $[Pu_{dis}]$ is the sum of Pu^{3+} ions and hydrolyzed species of Pu(III), as described by eq 9, ignoring the other oxidation states of dissolved Pu. The concentration of hydrolyzed species can be expressed using the formation constants, $[Pu^{3+}]$, and $[H^+]$ in eq 3, ${}^*\beta_n' = [Pu(OH)_n^{3-n}][H^+]^n/[Pu^{3+}]$, as described in the third term in eq 9; the solubility products were determined using eq 10, which is a modification of eq 4.

$$[Pu(III)_{dis}] = [Pu^{3+}] + \sum [Pu(OH)_n^{3-n}] = [Pu^{3+}]\left(1 + \sum {}^*\beta_n'/[H^+]^n\right) \quad (9)$$

and

$${}^*K_{s,0}' = \left\{[Pu(III)_{dis}]/\left(1 + \sum {}^*\beta_n'/[H^+]^n\right)\right\}/[H^+]^3 \quad (10)$$

All $[Pu^{3+}]$ and $[Pu(III)_{dis}]$ values quantified by spectrophotometry and LSC, respectively, in the near-neutral pH_c range are listed in Table A2 in the Appendix. To obtain the solubility products according to eq 10 at each temperature , the formation constants, ${}^*\beta_1'$ listed in Table 1 were applied with the exclusion of further hydrolysis species due to the lack of experimental results of ${}^*\beta_2'$ and ${}^*\beta_3'$ for Pu(III)−OH species at various temperatures. The solubility product at 25 °C obtained in our previous work[22] was recalculated considering pH_c, which was corrected using the experimentally acquired A_c factor in this work. The solubility products at various temperatures at the ionic strength of 0.1 M $NaClO_4$ and I = 0 are summarized in Table 2. A bluish precipitate at 25 °C was confirmed as $Pu(OH)_3$(am) based on the amorphous profile in the XRD spectrum.[22] In this work, however, the solid phase characterization could not be performed at varying temperatures due to the limited amount of Pu in stock. The formed $Pu(OH)_3$(s) is regarded as an amorphous solid based on the prior experimental result at 25 °C,[22] which was obtained under the same experimental conditions except for temperature.

Figure 5 shows log$[Pu(III)_{dis}]$ as a function of pH_c at 0.1 M $NaClO_4$ for the samples listed in Table A2. The closed and open symbols represent the calculated $[Pu(III)_{dis}]$ with $[Pu^{3+}]$ and ${}^*\beta_1'$ and the measured $[Pu(III)_{dis}]$ by LSC, respectively. The solubility curves are calculated with log ${}^*\beta_1'$ and log ${}^*K_{s,0}'$ listed in Tables 1 and 2 as a function of pH_c at each temperature.

https://doi.org/10.1021/acs.inorgchem.2c01590
Inorg. Chem. 2022, 61, 12643−12651

Table 2. Solubility Product, $Pu(OH)_3(am) + 3H^+ \rightleftharpoons Pu^{3+} + 3H_2O$, for $Pu(OH)_3(am)$, at 10, 17, 25, and 40 °C

temperature (°C)	log ${}^*K'_{s,0}$ (I = 0.1 M $NaClO_4$)	log ${}^*K^\circ_{s,0}$ (I = 0 M, SIT)	$\Delta_r H^\circ_m$ (kJ mol^{-1})	$\Delta_r S^\circ_m$ (J mol^{-1} K^{-1})
10	17.88 ± 0.64	17.24 ± 0.64		
17	16.05 ± 0.96	15.41 ± 0.96	−294.29 ± 23.05	−712.46 ± 78.39
25[a]	14.93 ± 0.50[a]	14.28 ± 0.50[a]		
40	12.78 ± 1.02	12.11 ± 1.02		

[a]Recalculated value from ref 22.

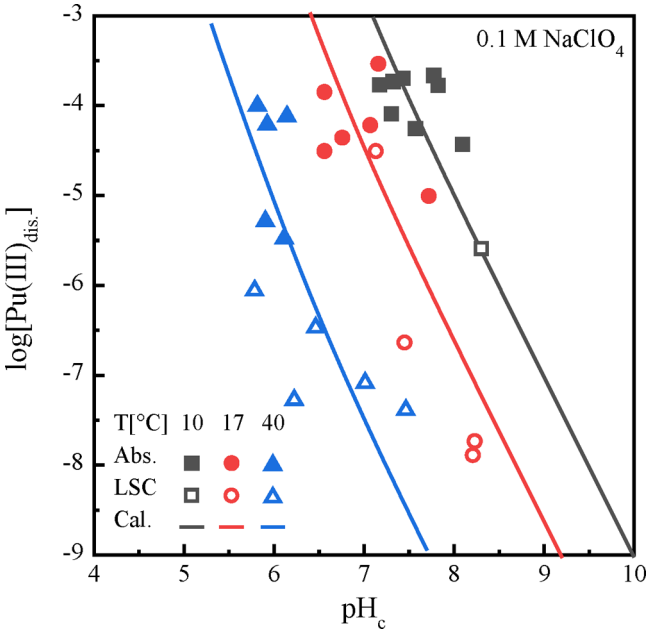


Figure 5. Solubility data and curves of $Pu(OH)_3(am)$ determined at various temperatures (T = 10, 17, and 40 °C) in 0.1 M $NaClO_4$. Symbols represent the experimentally determined log[$Pu(III)_{dis}$], and lines are calculated with ${}^*\beta'_1$ and ${}^*K'_{s,0}$ (I = 0.1 M $NaClO_4$) obtained in the present work.

Thermodynamic Data Evaluation. The linear correlation of the logarithmic equilibrium constants with the reciprocal absolute temperature (1/K) is shown in Figure 6. Standard molal enthalpy and entropy of reactions were derived according to the van't Hoff equation, eq 7, from the slope ($\Delta_r H^\circ_m$ = −slope × R × ln 10) and intercept ($\Delta_r S^\circ_m$ = intercept × R × ln 10) of the linear regression results. $\Delta_r H^\circ_m$ and $\Delta_r S^\circ_m$ for the formation of $Pu(OH)^{2+}$ species and the dissolution of $Pu(OH)_3(am)$ are summarized in Tables 1 and 2, respectively. These thermodynamic parameters indicate that the hydrolysis of Pu(III) is an endothermic reaction ($\Delta_r H^\circ_m$ = 34.10 ± 4.48 kJ mol^{-1}). The exothermic characteristic of the dissolution of $Pu(OH)_3(am)$ ($\Delta_r H^\circ_m$ = −294.29 ± 23.05 kJ mol^{-1}) is validated by the decrease in solubility with increasing temperature, which is coincident with those for trivalent lanthanide elements [Ln(III)].[35−40] In the hydrolysis reaction, the net change of enthalpy and entropy is a combination effect of the dissociation of water molecules in the first hydration shell, the formation of Pu−OH, and the change in the hydration environment between Pu^{3+} and $Pu(OH)_n^{3-n}$ ions. The relatively large enthalpy change during the dissolution process can be ascribed to the energetically large contribution to the phase transition of the amorphous solid phase to the hydrated aqueous phase, $Pu(OH)_3(aq)$. The negative entropy change is validated by comparing 3 equiv of hydrogen ions as the reactant and 1 equiv of hydrated Pu^{3+} ions as the product.[41]

To the best of our knowledge, this study is the first to report experimentally determined enthalpy and entropy changes in the hydrolysis and dissolution of trivalent actinides (An(III)). The quantitative values of the reaction enthalpy and entropy changes for Pu(III) hydrolysis were evaluated by comparing them with those of Ln(III) hydrolysis. It is a practical alternative over the limited information on An(III), as An(III) and Ln(III) are generally known to share similar trends in chemical behavior.[42] The enthalpy−entropy compensation refers to a linear relationship between enthalpy and entropy changes of a series of reactions, which has been reported in a wide range of fields in

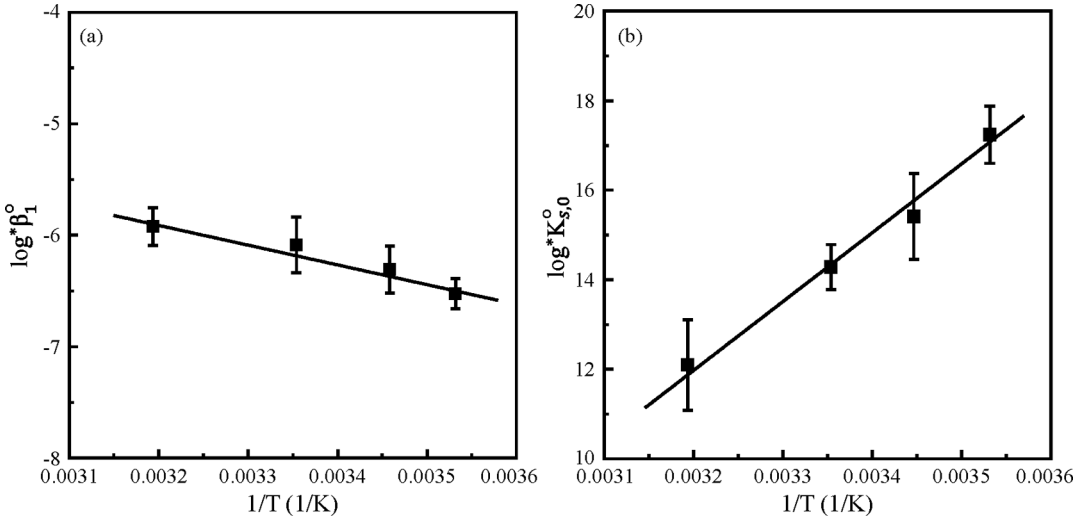


Figure 6. Plots of log ${}^*\beta^\circ_1$ (left) and log ${}^*K^\circ_{s,0}$ (right) versus $1/T$ and linear regression according to the integrated van't Hoff equation.

https://doi.org/10.1021/acs.inorgchem.2c01590
Inorg. Chem. 2022, 61, 12643−12651

chemistry to explain similarities between chemical reactions.[43] In actinide and lanthanide chemistry, similarity for An(III)/Ln(III) monofluoride complexation was discussed with the enthalpy−entropy compensation.[42] Figure 7 shows a linear

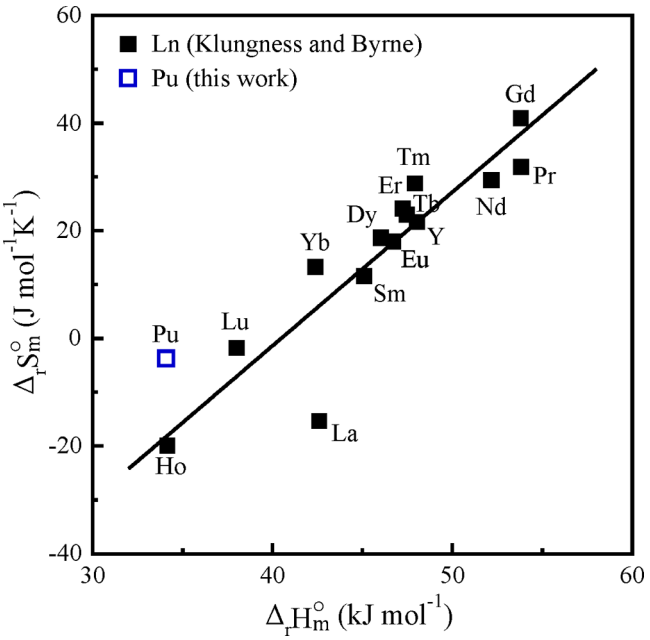


Figure 7. $\Delta_r H^\circ_m$ and $\Delta_r S^\circ_m$ of the first hydrolysis reaction for trivalent lanthanide show an enthalpy−entropy compensation, and the present results for the formation reaction of $Pu(OH)^{2+}$ species are comparable with the data for Ln(III).

relationship between the $\Delta_r H^\circ_m$ and $\Delta_r S^\circ_m$ of the first hydrolysis reaction for Ln(III) and the present Pu(III) hydrolysis data. $\Delta_r H^\circ_m$ and $\Delta_r S^\circ_m$ of Ln(III) were evaluated in this work using experimentally determined data at 20, 40, and 55 °C in 0.725 m $NaClO_4$ by Klungness and Byren.[35] These data, log ${}^*\beta_1'$, were listed as the recalculated values (referred to as "accepted") in a review paper by Brown and Ekberg.[36] The accepted log ${}^*\beta_1'$ values were converted to log ${}^*\beta_1^\circ$ at zero ionic strength by means of SIT with $\varepsilon(Ln^{3+}; ClO_4^-) = 0.49 \pm 0.05$ and $\varepsilon(Ln(OH)^{2+}; ClO_4^-) = 0.39 \pm 0.04$. The temperature-dependent Debye−Hückel terms (D) were treated identically, as described in the Experimental Section. $\Delta_r H^\circ_m$ and $\Delta_r S^\circ_m$ for Ln(III) were derived according to the van't Hoff equation, eq 7, with log ${}^*\beta_1^\circ$ (T = 20, 40, and 55 °C). As shown in Figure 7, the thermodynamic parameters for the first hydrolysis of Pu(III) were comparable to the linear enthalpy−entropy compensation for the first hydrolysis of Ln(III). To evaluate the compensation effect within the An(III) series, further thermodynamic studies on other An(III) ions, such as Am(III) and Cm(III), are encouraged. In the case of dissolution, a few studies on the solubility of $Ln(OH)_3$(cr) (Ln = La, Nd, and Gd) have been performed at temperatures ranging from 25 to 80 °C.[38−40] However, the amount of data is not sufficient to discuss the enthalpy and entropy relationship of the dissolution of $Ln(OH)_3$ and $Pu(OH)_3$(am).

CONCLUSIONS

In this study, the hydrolysis of Pu(III) and the dissolution of $Pu(OH)_3$(am) were investigated to determine the formation constants of the hydrolyzed species and the solubility product of $Pu(OH)_3$(am) as functions of temperature (10−40 °C) and thermodynamic parameters ($\Delta_r H^\circ_m$ and $\Delta_r S^\circ_m$). To determine the thermodynamic data for Pu(III) in aqueous solutions, Pu(III) was maintained by electrolysis; the hydrolysis was studied by the combination of sensitive absorption spectroscopy coupled with a capillary cell, LIBD, coulometric titration, and LSC at various temperatures. The standard reaction enthalpies and entropies of hydrolysis and dissolution were evaluated according to the van't Hoff equation. The hydrolysis of Pu(III) appeared to be endothermic with loss of entropy. It is energetically comparable to the hydrolysis of trivalent lanthanide elements. The $\Delta_r H^\circ_m$ and $\Delta_r S^\circ_m$ values for the dissolution of $Pu(OH)_3$(am) were exothermic with a relatively large loss of entropy. With respect to the radionuclide release scenarios in a deep underground repository, these thermodynamic data suggest that, at elevated temperatures, the hydrolysis of Pu(III) and precipitation of $Pu(OH)_3$(s) are facilitated, resulting in a decrease in dissolved Pu concentrations. This indicates that Pu migration through groundwater can be retarded at elevated temperatures. The inclusion of our thermodynamic data for geochemical modeling enables the simulation of elevated temperatures and thus improves the reliability of the safety assessment for the initial stage of HLRW disposal. The present data set provides a more comprehensive description of Pu hydrolysis chemistry under long-term evolution conditions, including gradual temperature variations around underground repositories.

APPENDIX

Table A1. Experimental Data for the Calculation of the First Hydrolysis Constant at Each Temperature (T = 10, 17, and 40 °C)

temperature (°C)	pH$_c$	[Pu^{3+}] (M)	[$Pu(OH)^{2+}$] (M)
10	5.68	4.33×10^{-5}	3.3×10^{-6}
	6.03	4.07×10^{-5}	5.9×10^{-6}
	5.07	4.70×10^{-5}	0.7×10^{-6}
	6.57	3.76×10^{-5}	9.9×10^{-6}
	6.61	3.57×10^{-5}	1.20×10^{-5}
	6.64	3.09×10^{-5}	1.68×10^{-5}
	6.16	1.48×10^{-4}	1.90×10^{-5}
	5.92	1.30×10^{-4}	1.4×10^{-5}
	6.18	1.33×10^{-4}	2.3×10^{-5}
	5.82	1.67×10^{-4}	1.7×10^{-5}
	5.93	1.68×10^{-4}	1.6×10^{-5}
	6.07	1.58×10^{-4}	2.6×10^{-5}
	5.62	4.55×10^{-5}	1.1×10^{-6}
17	4.90	5.04×10^{-5}	0.6×10^{-6}
	5.23	4.95×10^{-5}	1.2×10^{-6}
	5.41	4.79×10^{-5}	2.8×10^{-6}
	5.69	4.45×10^{-5}	6.2×10^{-6}
	5.80	4.29×10^{-5}	8.8×10^{-6}
	4.92	9.52×10^{-5}	2.8×10^{-6}
	5.47	9.60×10^{-5}	2.0×10^{-6}
	5.48	9.44×10^{-5}	3.6×10^{-6}
	5.25	4.58×10^{-5}	1.1×10^{-6}
	5.90	4.04×10^{-5}	6.5×10^{-6}
40	5.15	1.90×10^{-5}	1.5×10^{-6}
	5.37	1.91×10^{-5}	3.9×10^{-6}
	5.58	3.95×10^{-5}	5.5×10^{-6}
	5.84	3.53×10^{-5}	9.7×10^{-6}

https://doi.org/10.1021/acs.inorgchem.2c01590
Inorg. Chem. 2022, 61, 12643−12651

temperature (°C)	pH_c	$[Pu^{3+}]$ (M)	$[Pu(OH)^{2+}]$ (M)
	5.42	5.17×10^{-5}	4.4×10^{-6}
	5.11	9.05×10^{-5}	3.1×10^{-6}
	5.63	8.02×10^{-5}	1.34×10^{-5}

Table A2. Experimental Data for the Calculation of the Solubility Product at Each Temperature (10, 17, and 40 °C)

temperature (°C)	pH_c	$[Pu^{3+}]$ (M)	$[Pu(III)_{dis}]$ (M)
10	7.30	2.33×10^{-5}	
	8.09	2.3×10^{-6}	
	7.57	9.94×10^{-6}	
	7.17	5.98×10^{-5}	
	7.32	5.14×10^{-5}	
	7.43	4.60×10^{-5}	
	7.77	2.60×10^{-5}	
	7.82	1.81×10^{-5}	
	8.30		2.58×10^{-6}
17	6.56	8.14×10^{-5}	
	7.16	7.36×10^{-5}	
	7.07	1.78×10^{-5}	
	7.72	5.60×10^{-6}	
	6.56	4.80×10^{-5}	
	6.76	4.27×10^{-5}	
	8.21		1.29×10^{-8}
	8.23		1.84×10^{-8}
	7.45		2.31×10^{-7}
	7.13		3.12×10^{-5}
40	5.81	7.68×10^{-5}	
	5.90	3.8×10^{-6}	
	6.11	2.1×10^{-6}	
	6.14	4.65×10^{-5}	
	5.92	4.46×10^{-5}	
	5.78		8.77×10^{-7}
	6.46		3.39×10^{-7}
	7.01		8.22×10^{-8}
	6.22		5.3×10^{-8}
	7.46		4.1×10^{-8}

■ ASSOCIATED CONTENT

Supporting Information

The Supporting Information is available free of charge at https://pubs.acs.org/doi/10.1021/acs.inorgchem.2c01590.

Oxidation of Pu(III) according to pH and temperatures; experimentally determined factor A_c at 10, 17, 25, 33, and 40 °C; slope analysis for Pu(III) hydrolysis at 17 °C; and a description of LIBD results (PDF)

■ AUTHOR INFORMATION

Corresponding Author

Hye-Ryun Cho − *Nuclear Chemistry Research Team, Korea Atomic Energy Research Institute, Daejeon 34057, Republic of Korea; Department of Radiochemistry and Nuclear Nonproliferation, University of Science and Technology (UST), Daejeon 34113, Republic of Korea;* orcid.org/0000-0002-1293-6653; Phone: +82-42-868-8392; Email: hrcho@kaeri.re.kr

Authors

Sangki Cho − *Nuclear Chemistry Research Team, Korea Atomic Energy Research Institute, Daejeon 34057, Republic of Korea; Department of Radiochemistry and Nuclear Nonproliferation, University of Science and Technology (UST), Daejeon 34113, Republic of Korea*

Hee-Kyung Kim − *Nuclear Chemistry Research Team, Korea Atomic Energy Research Institute, Daejeon 34057, Republic of Korea;* orcid.org/0000-0001-5840-7194

Tae-Hyeong Kim − *Nuclear Chemistry Research Team, Korea Atomic Energy Research Institute, Daejeon 34057, Republic of Korea*

Wansik Cha − *Nuclear Chemistry Research Team, Korea Atomic Energy Research Institute, Daejeon 34057, Republic of Korea*

Complete contact information is available at: https://pubs.acs.org/10.1021/acs.inorgchem.2c01590

Author Contributions

The manuscript was written through the contributions of all authors. All the authors approved the final version of the manuscript.

Notes

The authors declare no competing financial interest.

■ ACKNOWLEDGMENTS

This study was supported by the Nuclear Research and Development Program of the National Research Foundation (NRF) of Korea (2017M2A8A5014719) and the Institute for Korea Spent Nuclear Fuel and NRF of Korea (2021M2E1A1085202).

■ REFERENCES

(1) *Overview of Eight Countries Overview of Eight Countries−Status*; Report 2019:1; Report for Swedish National Council for Nuclear Waste, April 2019.

(2) Jobmann, M.; Bebiolka, A.; Burlaka, V.; Herold, P.; Jahn, S.; Lommerzheim, A.; Maßmann, J.; Meleshyn, A.; Mrugalla, S.; Reinhold, K.; Rübel, A.; Stark, L.; Ziefle, G. Safety Assessment Methodology for a German High-Level Waste Repository in Clay Formations. *J. Rock Mech. Geotech. Eng.* **2017**, *9*, 856−876.

(3) Giffaut, E.; Grivé, M.; Blanc, P.; Vieillard, P.; Colàs, E.; Gailhanou, H.; Gaboreau, S.; Marty, N.; Madé, B.; Duro, L. Andra Thermodynamic Database for Performance Assessment: ThermoChimie. *Appl. Geochem.* **2014**, *49*, 225−236.

(4) Thoenen, T.; Hummel, W.; Berner, U.; Curti, E. *The PSI/Nagra Chemical Thermodynamic Database 12/07: Nuclear Energy and Safety Research Department Laboratory for Waste Management (LES)*; PSI, 2014.

(5) Kitamura, A. *JAEA-TDB-RN in 2020: Update of JAEA's Thermodynamic Database for Solubility and Speciation of Radionuclides for Performance Assessment of Geological Disposal of High-Level and TRU Wastes*; JAEA-Data/Code 2021; JAEA, 2020.

(6) Wanner, H. W. the NEA Thermochemical Data Base Project. *Radiochim. Acta.* **1988**, *44−45*, 325−330.

(7) Grenthe, I.; Gaona, X.; Plyasunov, A. V.; Rao, L.; Runde, W. H.; Grambow, B.; Konings, R. J. M.; Smith, A. L.; Moore, E. E. *Second Update on the Chemical Thermodynamics of Uranium: Neptunium, Plutonium, Americium and Technetium*; Ragoussi, M.-E., Martinez, J. S., Davide, C., Eds.; OECD, 2020.

(8) Metz, V.; Geckeis, H.; González-Robles, E.; Loida, A.; Bube, C.; Kienzler, B. Radionuclide Behaviour in the Near-Field of a Geological Repository for Spent Nuclear Fuel. *Radiochim. Acta.* **2012**, *100*, 699−713.

(9) Koke, C.; Skerencak-Frech, A.; Panak, P. J. Thermodynamics of the Complexation of Curium(III) with Chloride in Alkali and Alkali Earth Metal Solutions at Elevated Temperatures. *J. Chem. Thermodyn.* **2019**, *131*, 219−224.
(10) Jordan, N.; Demnitz, M.; Lösch, H.; Starke, S.; Brendler, V.; Huittinen, N. Complexation of Trivalent Lanthanides (Eu) and Actinides (Cm) with Aqueous Phosphates at Elevated Temperatures. *Inorg. Chem.* **2018**, *57*, 7015−7024.
(11) Maiwald, M. M.; Müller, K.; Heim, K.; Rothe, J.; Dardenne, K.; Rossberg, A.; Koke, C.; Trumm, M.; Skerencak-Frech, A.; Panak, P. J. Complexation of Np(V) with the Dicarboxylates, Malonate, and Succinate: Complex Stoichiometry, Thermodynamic Data, and Structural Information. *Inorg. Chem.* **2021**, *60*, 18674−18686.
(12) Maiwald, M. M.; Fellhauer, D.; Skerencak-Frech, A.; Panak, P. J. The Complexation of Neptunium(V) with Fluoride at Elevated Temperatures: Speciation and Thermodynamics. *Appl. Geochem.* **2019**, *104*, 10−18.
(13) Lee, J.-Y.; Amayri, S.; Montoya, V.; Fellhauer, D.; Gaona, X.; Altmaier, M. Solubility and Stability of Liebigite, $Ca_2UO_2(CO_3)_3 \cdot 10H_2O$(cr), in Dilute to Concentrated NaCl and $NaClO_4$ Solutions at T = 22−80 °C. *Appl. Geochem.* **2019**, *111*, 104374−104386.
(14) Endrizzi, F.; Gaona, X.; Zhang, Z.; Xu, C.; Rao, L.; Garcia-Perez, C.; Altmaier, M. Thermodynamic Description of U(VI) Solubility and Hydrolysis in Dilute to Concentrated NaCl Solutions at T = 25, 55 and 80 °C. *Radiochim. Acta.* **2019**, *107*, 663−678.
(15) Endrizzi, F.; Gaona, X.; Marques Fernandes, M.; Baeyens, B.; Altmaier, M. Solubility and Hydrolysis of U(VI) in 0.5 mol/kg NaCl Solutions at T = 22 and 80 °C. *J. Chem. Thermodyn.* **2018**, *120*, 45−53.
(16) Lee, J. Y.; Yun, J. I. Temperature-Dependent Hydrolysis Reactions of U(VI) Studied by TRLFS. *J. Nucl. Fuel Cycle Waste Technol.* **2013**, *1* (1), 65−73.
(17) Feiveson, H.; Mian, Z.; Ramana, M. V.; von Hippel, F. Spent Fuel from Nuclear Power Reactors: An Overview of a New Study by the International Panel on Fissile Materials. *Int. Panel Fissile Mater.* **2011**, 1−21.
(18) Hedin, A. *Spent Nuclear Fuel − How Dangerous Is It?* Technical Report SKB TR 97-13 for Swedish Nuclear Fuel and Waste Management Co, 1997.
(19) Schramke, J. A.; Santillan, E. F. U.; Peake, R. T. Plutonium Oxidation States in the Waste Isolation Pilot Plant Repository. *Appl. Geochem.* **2020**, *116*, 104561−104575.
(20) Neck, V.; Altmaier, M.; Fanghänel, T. Solubility of Plutonium Hydroxides/Hydrous Oxides under Reducing Conditions and in the Presence of Oxygen. *C. R. Chim.* **2007**, *10*, 959−977.
(21) Felmy, A. R.; Rai, D.; Schramke, J. A.; Ryan, J. L. The Solubility of Plutonium Hydroxide in Dilute Solution and in High-Ionic-Strength Chloride Brines. *Radiochim. Acta.* **1989**, *48*, 29−36.
(22) Cho, H. R.; Youn, Y. S.; Jung, E. C.; Cha, W. Hydrolysis of Trivalent Plutonium and Solubility of $Pu(OH)_3$ (Am) under Electrolytic Reducing Conditions. *Dalton Trans.* **2016**, *45*, 19449−19457.
(23) Tasi, A.; Gaona, X.; Fellhauer, D.; Böttle, M.; Rothe, J.; Dardenne, K.; Schild, D.; Grivé, M.; Colàs, E.; Bruno, J.; Källström, K.; Altmaier, M.; Geckeis, H. Redox Behavior and Solubility of Plutonium under Alkaline, Reducing Conditions. *Radiochim. Acta.* **2018**, *106*, 259−279.
(24) Morss, L. R.; Williams, C. W. Synthesis of Crystalline Americium Hydroxide, $Am(OH)_3$ and Determination of Its Enthalpy of Formation; Estimation of the Solubility-Product Constants of Actinide(III) Hydroxides. *Radiochim. Acta.* **1994**, *66*−*67*, 89−94.
(25) Ciavatta, L. The Specific Interaction Theory in Evaluating Ionic Equilibria. *Ann. Chim.* **1980**, *70*, 551.
(26) Hnedkovsky, L.; Hefter, G. Densities and Apparent Molar Volumes of Aqueous Solutions of $NaClO_4$, $KClO_4$, and KCl at Temperatures from 293 to 343 K. *J. Chem. Eng. Data* **2021**, *66*, 3645−3658.
(27) Baes, C. F., Jr; Mesmer, R. E. *The Hydrolysis of Cations*; Wiley Interscience: New York, 1976.
(28) Cho, H.-R.; Jung, E. C.; Park, K. K.; Song, K.; Yun, J. I. Effect of Reduction on the Stability of Pu(VI) Hydrolysis Species. *Radiochim. Acta.* **2010**, *98*, 555−561.
(29) Jung, E. C.; Cho, H.-R. Characteristics of the Laser-Induced Breakdown Detection of Colloidal Nanoparticles for Determining Particle Size. In *The Delivery of Nanoparticles*; INTECH, 2012; pp 431−452.
(30) Boström, M.; Craig, V. S. J.; Albion, R.; Williams, D. R. M.; Ninham, B. W. Hofmeister Effects in PH Measurements: Role of Added Salt and Co-Ions. *J. Phys. Chem. B* **2003**, *107*, 2875−2878.
(31) Altmaier, M.; Metz, V.; Neck, V.; Müller, R.; Fanghänel, T. Solid−Liquid Equilibria of $Mg(OH)_2$(cr) and $Mg_2(OH)_3Cl \cdot 4H_2O$(cr) in the System Mg-Na-H-OH-Cl-H_2O at 25°C. *Geochim. Cosmochim. Acta* **2003**, *67*, 3595−3601.
(32) Puigdomènech, I.; Rard, J. A.; Plyasunov, A. V.; Grenthe, I. *TDB-4 Temperature Corrections to Thermodynamic Data and Enthalpy Calculations*. Report for Agence de L'OCDE pour L'Energie Nucléaire, 1999.
(33) Cohen, D. The Absorption Spectra of Plutonium Ions in Perchloric Acid Solutions. *J. Inorg. Nucl. Chem.* **1961**, *18*, 211−218.
(34) Neck, V.; Fanghänel, T.; Rudolph, G.; Kim, J. I. Thermodynamics of Neptunium(V) in Concentrated Salt Solutions: Chloride Complexation and Ion Interaction (Pitzer) Parameters for the NpO_2^+. *Radiochim. Acta.* **1995**, *69*, 39−48.
(35) Klungness, G. D.; Byrne, R. H. Comparative Hydrolysis Behavior of the Rare Earths and Yttrium: The Influence of Temperature and Ionic Strength. *Polyhedron.* **2000**, *19*, 99−107.
(36) Brown, P. L.; Ekberg, C. *Hydrolysis of Metal Ions*; John Wiley & Sons, 2016.
(37) İçhedef, Ç.; Şişmanoğlu, T.; Teksöz, S. Hydrolytic Behavior of La^{3+} and Sm^{3+} at Various Temperatures. *J. Solution Chem.* **2018**, *47*, 220−230.
(38) Moniruzzaman, M.; Kobayashi, T.; Sasaki, T. Solubility and Solid Phase of Trivalent Lanthanide Hydroxides and Oxides. *J. Nucl. Radiochem. Sci.* **2020**, *20*, 32−42.
(39) Wood, S. A.; Palmer, D. A.; Wesolowski, D. J.; Bénézeth, P. The Aqueous Geochemistry of the Rare Earth Elements and Yttrium. Part XI. The Solubility of Nd $(OH)_3$ and Hydrolysis of Nd^{3+} from 30 to 290 C at Saturated Water Vapor Pressure with in-Situ pH_m Measurement. In *Water−Rock Interactions, Ore Deposits, and Environmental Geochemistry: A Tribute to David A Crerar*; The Geochemical Society, 2002; Vol. 7, pp 229−256.
(40) Deberdt, S.; Castet, S.; Dandurand, J.-L.; Harrichoury, J.-C.; Louiset, I. Experimental Study of $La(OH)_3$ and $Gd(OH)_3$ Solubilities (25 to 150°C), and La−Acetate Complexing (25 to 80°C). *Chem. Geol.* **1998**, *151*, 349−372.
(41) Saha, D.; Mukherjee, A. Impact of Ions on Individual Water Entropy. *J. Phys. Chem. B* **2016**, *120*, 7471−7479.
(42) Choppin, G. R. Comparison of the Solution Chemistry of the Actinides and Lanthanides. *J. Less Common Met.* **1983**, *93*, 323−330.
(43) Liu, L.; Guo, Q. X. Isokinetic Relationship, Isoequilibrium Relationship, and Enthalpy−Entropy Compensation. *Chem. Rev.* **2001**, *101*, 673−695.

https://doi.org/10.1021/acs.inorgchem.2c01590
Inorg. Chem. 2022, 61, 12643−12651